

Sphingosine-1-Phosphate Activates the AKT Pathway to Protect Small Intestines from Radiation-Induced Endothelial Apoptosis

Stéphanie Bonnaud¹, Colin Niaudet¹, François Legoux¹, Isabelle Corre¹, Gregory Delpon², Xavier Saulquin¹, Zvi Fuks³, Marie-Hélène Gaugler^{1,4}, Richard Kolesnick⁵, and François Paris^{1,2}

Abstract

A previous *in vitro* study showed that sphingosine-1-phosphate (S1P), a ceramide antagonist, preserved endothelial cells in culture from radiation-induced apoptosis. We proposed to validate the role of S1P in tissue radioprotection by inhibiting acute gastrointestinal (GI) syndrome induced by endothelial cell apoptosis after high dose of radiation. Retro-orbital S1P was injected in mice exposed to 15 Gy, a dose-inducing GI syndrome within 10 days. Overall survival and apoptosis on intestines sections were studied. Intestinal cell type targeted by S1P and early molecular survival pathways were researched using irradiated *in vitro* cell models and *in vivo* mouse models. We showed that retro-orbital S1P injection before irradiation prevented GI syndrome by inhibiting endothelium collapse. We defined endothelium as a specific therapeutic target because only these cells and not intestinal epithelial cells, or B and T lymphocytes, were protected. Pharmacologic approaches using AKT inhibitor and pertussis toxin established that S1P affords endothelial cell protection *in vitro* and *in vivo* through a mechanism involving AKT and 7-pass transmembrane receptors coupled to Gi proteins. Our results provide strong pharmacologic and mechanistic proofs that S1P protects endothelial cells against acute radiation enteropathy. *Cancer Res*; 70(23); 9905–15. ©2010 AACR.

Introduction

Research has shed new light on the critical role of microvasculature collapse in tissue pathology induced by genotoxic stresses (1). A notable, but controversial, example is the involvement of microvascular endothelium in the early response to radiation. The gastrointestinal (GI) syndrome, an acute adverse effect of radiotherapy, has long been considered to be dependent solely on the dysfunction of the intestinal clonogenic compartment (2, 3). According to this single-target hypothesis, irradiation at doses of 8 Gy or greater causes rapid stem cell apoptosis at positions 4 and 5 from the base of the crypt, followed by a mitotic catastrophe 24 to 48

hours postirradiation inhibiting crypt and villi regeneration. We and others challenged this single cell target model arguing for a more complex multitarget scenario. Microvascular endothelial apoptosis after single high dose of radiation constitutes a primary lesion, which contributes to stem cell dysfunction, crypt damage, villi denudation, organ failure, and death by GI syndrome (1, 4–6). This syndrome was prevented when endothelial cell apoptosis was pharmacologically inhibited in mice by intravenous injection of basic fibroblast growth factor (bFGF; ref. 1), an agonist of Toll-like receptor 5 (4) or angiopoietin-I (5) prior to irradiation.

Endothelial cell apoptosis is also triggered by ceramide, a sphingolipid generated upon hydrolysis of cell membrane sphingomyelin by acid sphingomyelinase (ASM; ref. 7). Genetic invalidation of ASM in mice inhibited the radiation-induced apoptosis of the microvascular endothelial cells (1), which inhibited GI syndrome and switched the death of the mouse to bone marrow (BM) aplasia. Sphingosine-1-phosphate (S1P) is a product of ceramide deacylation and phosphorylation of the sphingosine. Both S1P and ceramide, which have opposing properties, determine cell fate (8). Although ceramide is a proapoptotic factor, S1P promotes survival by activating the PI3K (phosphoinositide 3-kinase)/AKT pathway (9). S1P signaling may act either intracellularly through yet unidentified receptor(s) (10) or extracellularly through binding to G protein-coupled receptors termed S1P receptors (11). Inhibition of ceramide-induced apoptosis by S1P has been shown in several cell lines of different origins, such as lymphocytes and tumor cells (8), and has been

Authors' Affiliations: ¹Inserm UMR892-Centre de Recherche en Cancérologie Nantes-Angers, Nantes, France; ²Centre de Lutte Contre le Cancer Nantes-Atlantique, Saint-Herblain, France; ³Radiation Oncology Department, Memorial Sloan-Kettering Cancer Center, New York, New York; ⁴Institut de Radioprotection et de Sûreté Nucléaire, Fontenay-aux-Roses, France; and ⁵Laboratory of Signal Transduction, Sloan-Kettering Institute, New York, New York

Note: Supplementary data for this article are available at Cancer Research Online (<http://cancerres.aacrjournals.org/>).

S. Bonnaud and C. Niaudet contributed equally to the manuscript.

Corresponding Author: François Paris, Inserm UMR892-Centre de Recherche en Cancérologie Nantes-Angers, 8 quai Moncousu, 44007 Nantes, France. Phone: 33-228-080302; Fax: 33-228-080204; E-mail: francois.paris@inserm.fr.

doi: 10.1158/0008-5472.CAN-10-2043

©2010 American Association for Cancer Research.

confirmed *in vivo*. Administration of S1P 2 hours prior to exposure to 0.1 Gy protects almost the entire ovarian follicle population in mice, therefore preventing radiation-induced sterility (12).

S1P is already known to modulate endothelial functions, such as attenuate increase in vascular permeability by regulating junctional complexes (13). It has also been shown to block *in vitro* endothelial cell death induced by H₂O₂ (14), ethanol (15), and serum deprivation (16). We recently showed that S1P protects human microvascular endothelial cells (HMEC-1) from radiation-induced apoptosis (17). S1P acted directly on the ceramide-mediated death, but not on radiation-induced DNA damage pathway, to protect endothelial cells from ionizing radiation. In the present study, we propose to validate the role of exogenous S1P as a relevant bioactive lipid both to promote endothelial cell survival and to inhibit *in vivo* one of the radiation-induced intestinal pathologies (e.g., GI syndrome). To clarify the involvement of the endothelium in the GI syndrome, we sought to determine which cell types and molecular events of the survival pathway are preferentially targeted by S1P.

Materials and Methods

Cell lines, irradiation, and drug protocols

HMEC-1 and IEC-6 (intestinal epithelial cells) were kindly provided by F.J. Candal (Center for Disease Control) and M. Neunlist (Inserm UMR913, Nantes). Both were seeded at 2×10^4 cells/cm² as described (17, 18). Irradiation was carried out in a Faxitron CP160 irradiator (Faxitron X-ray Corporation) at a dose rate of 1.48 Gy/min. S1P [(1 μM) in PET vehicle (12); Biomol], Ly294002 (1 μmol/L in DMSO; Biomol) and pertussis toxin (PTx; 100 ng/mL in H₂O; Sigma) were respectively added 2, 2.5, and 3 hours before irradiation with low serum media (0.1% FBS).

Clonogenic and cell counting assays

For clonogenic studies, IEC-6 seeded at 2.5×10^3 cells per 60-mm dish were treated with or without (w/o) S1P and irradiated at 2 to 15 Gy. After 2 weeks, colonies were scored after staining with 1% Giemsa. Apoptotic HMEC-1 and IEC-6 floating in the medium were counted as described (17).

Apoptosis by APO 2.7 and caspase 3/7 assays

Apoptosis was assessed using the APO2.7 marker as previously described (17). For the caspase 3/7 assay, proteins (50 μg) diluted in 32 μL of caspase buffer (Promega) were incubated with 250 μmol/L of Ac-DEVD-AMC. Peptide cleavage was measured every 15 minutes over 2 hours using a fluorescent plate reader (Dynatech) at excitation and emission wavelengths of 365 and 465 nm, respectively. Specific caspase activity was expressed in nanomoles of AMC released per microgram of proteins.

Studies on immune cells

Peripheral blood mononuclear cells (PBMC) from healthy donors were maintained in RPMI-1640 medium. Cells were incubated w/o 1 μmol/L of S1P 2 hours before irradiation.

Cells (5×10^5) harvested at different time points postirradiation were hybridized with amcyan-CD3 or APC-CD19 (BD), FITC-Annexin V (Beckman Coulter), and 7-AAD (BD) and then processed using a FACS Canto II system (BD). Data were analyzed with FACS Diva 6.1 software (BD).

Western blotting

After lysis, S1P- and/or PTx-treated HMEC-1 proteins were separated by SDS-PAGE and transferred to ImmobilonP membrane (Millipore). The membrane was hybridized with antibodies of interest diluted at 1/1,000 for phospho-AKT (clone 9271; Cell Signaling), 1/1,000 for total AKT (clone 9272; Cell Signaling), and 1/2,500 for actin (Santa Cruz).

Animal, irradiation, and drug protocols

Eight- to 12-week-old C57Bl/6 male mice (Charles River) were housed in our animal core facility according to ongoing national regulations issues by INSERM and the French Department of Agriculture. Whole-body irradiation (WBR) was delivered with a ⁶⁰Co irradiator (Atomic Energy Canada) at 1 Gy/min. BM transplantation was carried out as described (19). After defining the maximum tolerated dose (MTD), 100 μg/25 g mouse of S1P in 0.2 mL of PET was injected intravenously in mice 30 minutes prior to and 5 minutes after irradiation. PTx (1 μg/25 g mouse) into 0.2 mL Hank's solution was injected intraperitoneally 2 hours and 30 minutes prior to, as well as 5 minutes and 2 hours, postirradiation. After defining the MTD, 10 μg/25 g mouse of AKT inhibitor XI (AKTi; Merck) in 0.2 mL of water was injected intravenously in mice 30 minutes prior to and 5 minutes after irradiation.

Mice survival, leukocytes counting, and cause of death

Actuarial survival was calculated by the Kaplan–Meier product limit method. Leukopenia was measured using hematology analyzer (Melet-Schloesing) after harvesting peripheral blood from irradiated and/or S1P-treated mice. Causes of death were evaluated by autopsy (1). Five-micrometer sections of duodenal and femoral segments from terminally ill animals were stained with hematoxylin/eosin (H&E). GI damage and BM aplasia were diagnosed when the small intestines displayed denuded mucosa with no villus and no apparent crypts and the marrow showed complete depletion of hematopoietic elements, respectively.

Crypt survival assay and epithelial cell death

Crypt survival assay (crypt colony count) was carried out on proximal duodenum harvested 3.5 days after irradiation as described (20). Surviving crypts per intestines cross section were defined as containing at least 10 adjacent chromophilic cells and 1 Paneth cell, as well as a lumen. Ten circumferences scored in 4 mice were used to generate each data point. Assessment of crypt epithelial cell death on small intestines harvested 24 hours after irradiation was done as described (3). Dead crypt cells, characterized by abnormal nucleus and/or appearance of micro-nuclei, were counted in 150 crypts scored in 4 mice.

Immunohistology

Endothelial apoptosis was assessed in 5-μm intestines sections by FITC- or peroxidase-labeled TUNEL, as previously

described protocol (1). Apoptotic cells were counted as described (1). Phospho-AKT (736E11; Cell Signaling) and FITC-CD31 antibodies (MEC13.3; BD Biosciences) at 1/50 and 1/200 dilution, respectively, were incubated overnight at 4°C after antigen was released by microwave heating in 0.1N citrate solution. Phospho-AKT was detected after hybridization with rhodamine-conjugated anti-rabbit antibody (BioSys), diluted at 1/200. Slides counterstained with 0.1 $\mu\text{mol/L}$ of 4',6-diamidino-2-phenylindole (DAPI; Sigma) were examined by standard (Axiovert 200; Carl Zeiss) or confocal (Leica) microscopy for colocalization studies.

Statistical analysis

Statistical analyses, the Student *t* test (95% confidence interval), and the Mantel log-rank test for survival were conducted using StatView 6.0.

Results

S1P rescues mice from radiation-induced GI syndrome

The ability of S1P to protect mice from radiation-induced death was estimated by overall survival. WBR of 15 Gy killed 100% of C57Bl/6 mice within 7 days, with a median survival time of 5 days (Fig. 1A). Two retro-orbital injections of S1P delayed significantly animal death by 4 days (median survival time of 9 days; $P < 0.01$ vs. 15 Gy). Autopsies on agonal animal, which died 5 days after exposure to 15 Gy, showed severe GI damage (e.g., GI syndrome), characterized by an absence of crypt/villus units and an inflamed but preserved BM (Fig. 1B). Contrastingly, autopsies of S1P-treated mouse, which died 9 days after irradiation, suffered from BM depletion whereas intestinal villi and crypts were preserved. Irradiated animals died from BM aplasia after S1P-injection instead of GI syndrome after sham treatment.

To determine the ability of S1P to inhibit intestinal apoptosis, TUNEL assays were done on duodenal sections from mice 4 hours after 15-Gy WBR w/o S1P (Fig. 1C). High amount of apoptotic cells (brown staining) was observed within the lamina propria from irradiated mice but not in the epithelium monolayer. S1P pretreatment inhibited radiation damage by reducing the amount of apoptotic cells within the lamina propria. Staining for FITC-TUNEL (green) and rhodamine-CD31 (red) in intestinal sections from 15 Gy-irradiated mice revealed colocalization of apoptotic and endothelial markers as shown by the yellow staining on the merged image (Fig. 1D). CD31, but not the TUNEL, remained visible in intestinal sections from S1P-treated and irradiated mice. S1P inhibited endothelial cell apoptosis compared with sham-irradiated condition (mean of endothelial cell apoptosis per villus \pm SEM 11.3 \pm 0.8% after 15 Gy vs. 3.7 \pm 0.5% after 15 Gy+S1P; Fig. 1E) and dramatically reduced the percentage of severely damaged villi containing more than 20 apoptotic cells (23.4% after 15 Gy vs. 1.3% after 15 Gy FITC + FITC S1P).

S1P enhances crypt radioprotection but not *in vitro* epithelial cell radioresistance

To better define cellular mode of action of S1P in GI syndrome protection, crypt survival assay was conducted in mice 3.5 days after S1P treatment and exposure to a range of

ionizing radiation dose. The number of crypts per duodenal circumference sections decreased in a dose-dependent manner (Fig. 2A). After 15 Gy, less than 1 crypt per circumference was quantifiable ($0.6 \pm 0.3\%$). S1P pretreatment dramatically enhanced crypt survival ($3.5 \pm 1.4\%$; $P < 0.01$ vs. 15 Gy), reaching an isoeffect close to 13 Gy + vehicle. Crypt radioprotection by S1P was confirmed by the fact that number of epithelial mitotic catastrophe per crypt decreased in S1P-treated mice (2.3 ± 0.1 24 hours after 15 Gy vs. 1.3 ± 0.1 after 15 Gy + S1P; $P < 0.01$; Fig. 2B). However, neither clonogenic survival nor early radioprotection was enhanced *in vitro* by S1P treatment of 15 Gy-irradiated IEC-6 primary epithelial cells as supported by the 50% of clonogenic survival (DL_{50} of 3.2 and 4.2 Gy for vehicle- and S1P-treated groups, respectively; Fig. 2C) and by apoptosis (Fig. 2D; $P > 0.1$ S1P vs. sham treatment at 24 and 48 hours postirradiation).

BM and lymphoid compartments are not protected by S1P after irradiation

WBR induces BM aplasia with severe leukopenia. The ability of S1P to protect lymphoid cells from radiation-induced death has been investigated using human PBMCs. Using multiparametric FACS analysis with amcyan-CD3, FITC-Annexin V, and 7-AAD (Fig. 3A), we showed that radiation-induced death increased similarly in T lymphocytes treated w/o S1P in a time-dependent manner (72 hours: $50.5 \pm 13.4\%$ after 15 Gy and $47.3 \pm 7.3\%$ after 15 Gy + S1P; $P > 0.1$; Fig. 3B). FACS analysis with APC-CD19, FITC-Annexin V, and 7-AAD (Fig. 3C) showed that B lymphocytes were more radiosensitive than T lymphocytes; however, no specific protection by S1P pretreatment was observed (24 hours: $57 \pm 10\%$ after 15 Gy and $58.3 \pm 10.5\%$ after 15 Gy + S1P; $P > 0.1$; Fig. 3D). To confirm the lack of radioprotection on hematopoietic cells by S1P, leukocytes were counted directly in irradiated mice on a daily basis. A slightly increase in the number of white blood cells was observed in sham-irradiated mice; however, leukocyte counts in irradiated mice were shown to decrease dramatically in a time-dependent manner, regardless of S1P treatment (day 4: $0.2 \pm 0.1\%$ after 15 Gy vs. $0.2 \pm 0.1\%$ after 15 Gy + S1P; $P > 0.1$; Fig. 3E). Agonal mice treated with 15 Gy + S1P presented severe leukopenia and BM aplasia. Autologous BM transplantation 16 hours after 15 Gy WBR and S1P treatment definitely explained the demise of the animals. If 15 Gy + BM-treated mice and 15 Gy-irradiated mice died within the time frame (median survival: 5 days after 15 Gy; 6 days after 15 Gy + BM; $P > 0.1$); however, cotreatment with S1P + BM increased survival of irradiated mice. Half of S1P- and BM-treated mice stayed alive 100 days postirradiation (median survival time: 9 days after 15 Gy + S1P; >100 days after 15 Gy + S1P + BM; $P < 0.01$). Surviving mice exhibited normal activity without any gross dysfunction, except fur depigmentation due to irradiation, until death that occurred suddenly 4 months postirradiation.

S1P-mediated radioprotection acts through the extracellular pathway

To validate our hypothesis that G-coupled protein receptors play a role for in the S1P-mediated endothelial

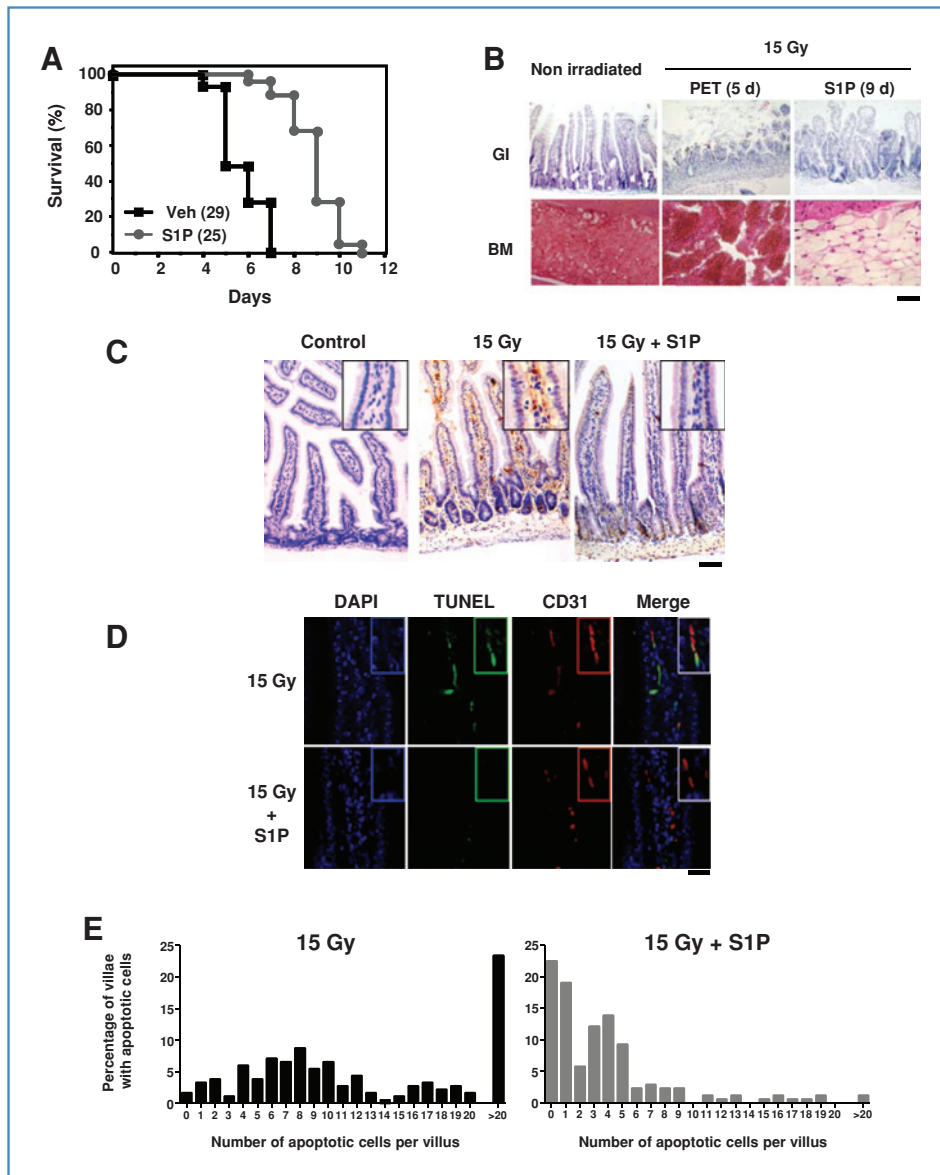


Figure 1. S1P treatment rescues from endothelial cell apoptosis-induced death mediated by high dose of radiation. A, survival curves of PET- or S1P-treated mice after 15-Gy WBR. Number in parentheses indicates animals per group. B, H&E-stained sections of proximal duodenum and femur from agonal animals after 15 Gy w/o S1P. Number in parentheses indicates the day postexposure to radiation when tissues have been harvested from the agonal animals. Scale bar, 250 μ m. C, apoptosis in duodenum 4 hours after 15 Gy w/o S1P. Apoptosis was evaluated by peroxidase-TUNEL (brown) counterstained with hematoxylin (blue). Scale bar, 100 μ m. D, colocalization between apoptotic FITC-TUNEL (green) and endothelial rhodamine-CD31 (red) shown by the yellow staining on the merge image and counterstained with DAPI (blue). Scale bar, large picture 60 μ m, window 30 μ m. E, apoptotic cell distribution by crypt/villus unit in duodenum after 15 Gy w/o S1P.

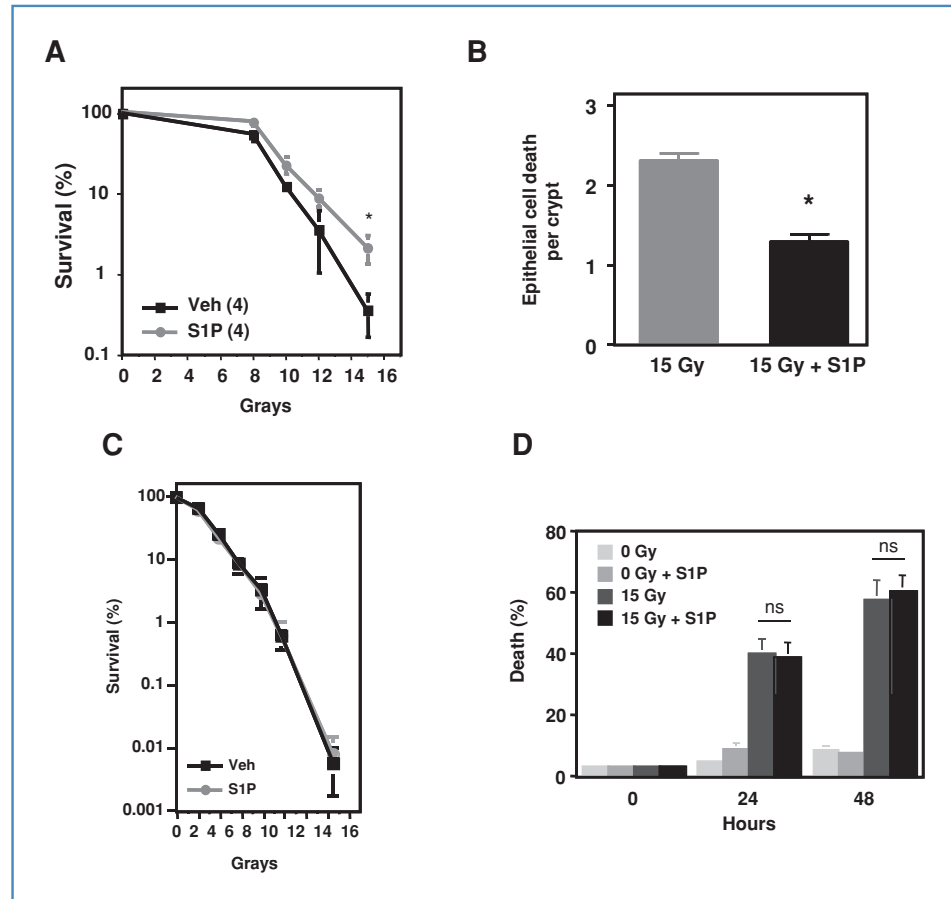
radioprotection, HMEC-1 were treated with PTx, which caused the uncoupling of Gi proteins from the S1P receptors, before treatment with S1P and exposure to 15 Gy. Radiation-induced death was inhibited by S1P ($32.7 \pm 6.3\%$ after 15 Gy vs. $13.6 \pm 2.6\%$ after 15 Gy + S1P; $P = 0.01$; Fig. 4A); however, PTx treatment restored apoptosis in S1P-treated endothelial cells to the level observed with exposure to 15 Gy alone ($23.4 \pm 4.4\%$ after 15 Gy + PTx + S1P, $P > 0.1$ vs. 15 Gy). Moreover, treatment with PTx alone did not modulate HMEC-1 radiosensitivity ($28.6 \pm 5.4\%$, $P > 0.1$ vs. 15 Gy), which suggests a direct inhibition of the S1P survival pathway. Inhibition of S1P-induced endothelial cell survival by PTx was confirmed by APO2.7 FACS analysis (Fig. 4B) and by a DEVDase assay (Fig. 4C). We then tested whether endothelial cell survival in the small intestines was enhanced by S1P through an extracellular mechanism (Fig. 4D). Injection of PTx prior to

a 15-Gy WBR did not modify mice survival as compared with that of sham-irradiated mice. However, PTx restored the radiosensitivity pattern in mice pretreated with S1P (median survival time: 8 days after 15 Gy + S1P and 5 days after 15 Gy + PTx + S1P; $P < 0.02$) and caused animals to die from GI syndrome in PTx- and S1P-treated mice instead of BM aplasia in the S1P-treated cohort (Fig. 4E). As determined by the TUNEL assay, PTx restored apoptotic cell pattern (green fluorescence) within the small intestines of S1P-treated and irradiated mice (Fig. 4F).

AKT phosphorylation is necessary in S1P-mediated intestinal radioprotection

AKT phosphorylation activates a robust survival signal that inhibits endothelial cell apoptosis. Western blot from S1P-treated HMEC-1 confirmed AKT phosphorylation

Figure 2. S1P does not protect intestinal epithelial cell from radiation exposure. A, crypt survival assay on transverse cross-section slides from duodenum harvested 3.5 days after WBR between 2 and 15 Gy w/o S1P. Surviving crypts for 10 H&E-stained circumferences (mean \pm SD, $n = 4$, *, $P < 0.01$). B, dead epithelial cells per crypt for 150 duodenal crypts 24 hours after 15 Gy (mean \pm SEM, $n = 3$, *, $P < 0.01$). C, clonogenic assay of vehicle- or S1P-treated IEC-6 before irradiation between 2 and 15 Gy. Irradiated clonogenic fraction was normalized to the nonirradiated clonogenic fraction (mean \pm SEM; $n = 3$ in duplicate, $P > 0.1$). D, death estimated by apoptotic floating cell counts in 15 Gy-irradiated IEC-6 treated w/o S1P (mean \pm SD; $n = 3$ in triplicate); ns, nonsignificant difference.



within 15 minutes (Fig. 5A), which was inhibited by PTx pretreatment. These results were also confirmed *in vivo*. Pretreatment with S1P, but not S1P + PTx, induced AKT phosphorylation in mice within 15 minutes, specifically within the lamina propria (Fig. 5B). Colocalization of rhodamine- α -phospho-AKT (red) and FITC-CD31 (green) into intestinal cross sections of S1P-treated mice, as shown by the yellow stain of the merged image (Fig. 5C), proves that S1P specifically induced AKT activation in the endothelial cells. To show the key role of AKT activation in S1P-mediated endothelial survival, HMEC-1 cells were pretreated with LY290004 prior to S1P treatment and 15-Gy exposure. PI3K inhibitor alone did not modulate HMEC-1 sensitivity ($27 \pm 6\%$ after 15 Gy + LY290004 vs. $23.1 \pm 3.4\%$ after 15 Gy; $P > 0.1$; Fig. 6A); however, LY290004 inhibited S1P-mediated radioprotection ($23.8 \pm 6.5\%$ after 15 Gy + S1P + LY290004 vs. $14.5 \pm 1.1\%$ after 15 Gy + S1P; $P < 0.1$). Inhibition of S1P-induced radioprotection by LY290004 was confirmed by APO2.7 FACS analysis (Fig. 6B). We then tested the ability of AKT inhibition to reverse radioprotection in our murine GI syndrome model. Pharmacologic action of water-soluble AKTi was proven by disappearance of rhodamine staining for phospho-AKT, detectable within the intestines of S1P-treated mice (Fig. 6C). Injection of AKTi did not modify mice survival as compared with sham-irradiated mice (Fig. 6D) but reduced survival time of S1P-treated and

irradiated mice (median survival time: S1P = 8 days; AKTi + S1P = 6 days; $P < 0.01$). As expected, animals died from GI syndrome in AKTi- and S1P-treated mice instead of BM aplasia in the S1P-treated cohort (Fig. 6E).

Discussion

Recent studies have shed new light on the critical role of the microvasculature in the regulation of tissue response to stresses. Endothelial cell apoptosis is initiated by activation/relocation of ASM-inducing ceramide generation leading to caspase activation. S1P, a ceramide antagonist, can protect quiescent endothelial cells in culture from radiation-induced apoptosis (17). In the present study, we establish S1P as a new, relevant, bioactive lipid acting to prevent endothelial apoptosis and acute organ necrosis in radiation-induced GI syndrome.

Very recently, the role of endothelial cell apoptosis in the pathogenesis of GI syndrome has been challenged. Mice selectively deleted not only for the apoptotic *bax* gene in hematopoietic and endothelial cells through Tie2Cre-loxP system but also for the apoptotic *bak1* gene in their whole genome (Tie2Cre;*bak1*^{-/-};*bax*^{FL/FL}) were not shown as more resistant to high dose radiation than the control (*bak1*^{-/-}; *bax*^{+/+}) mice. Unfortunately, invalidation of *bak1* in mice

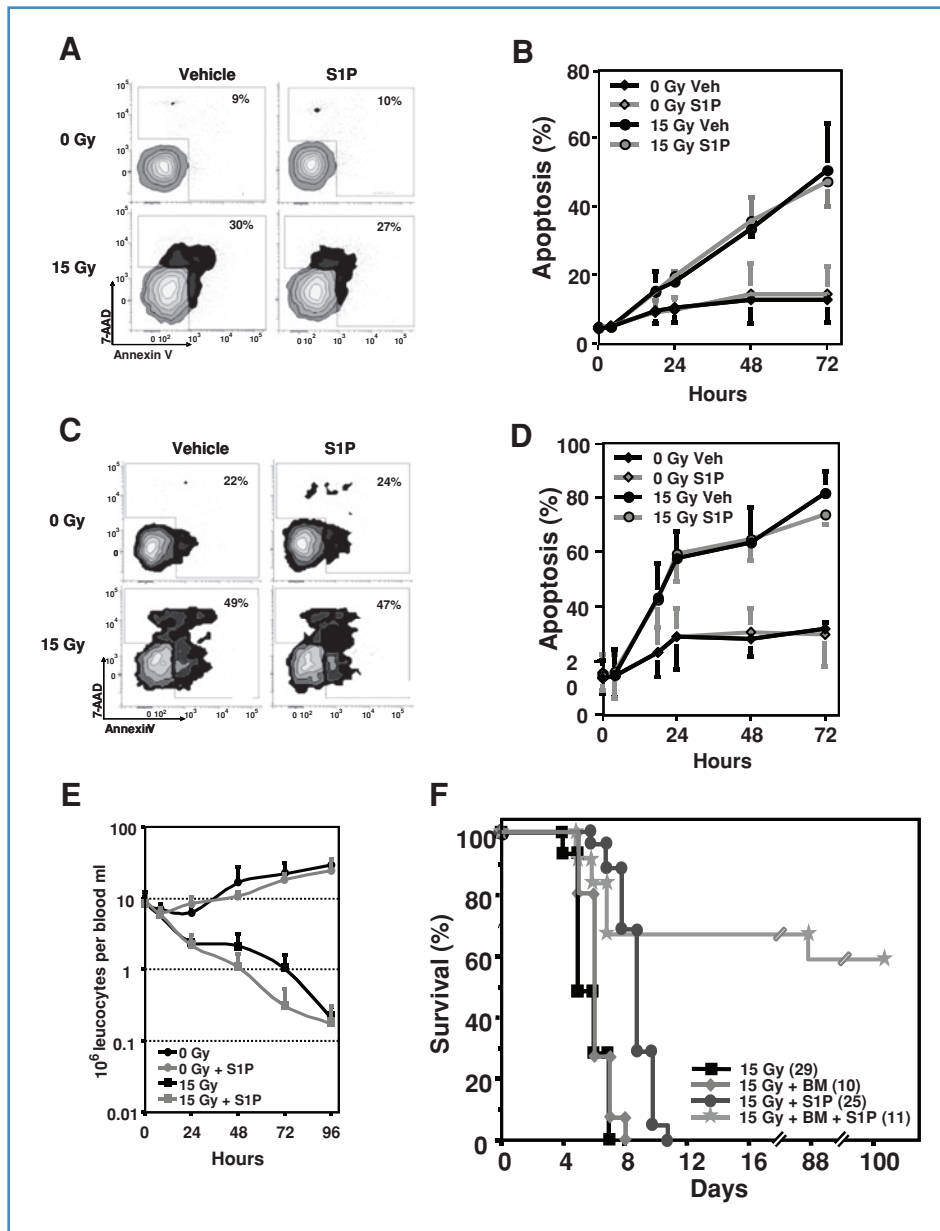


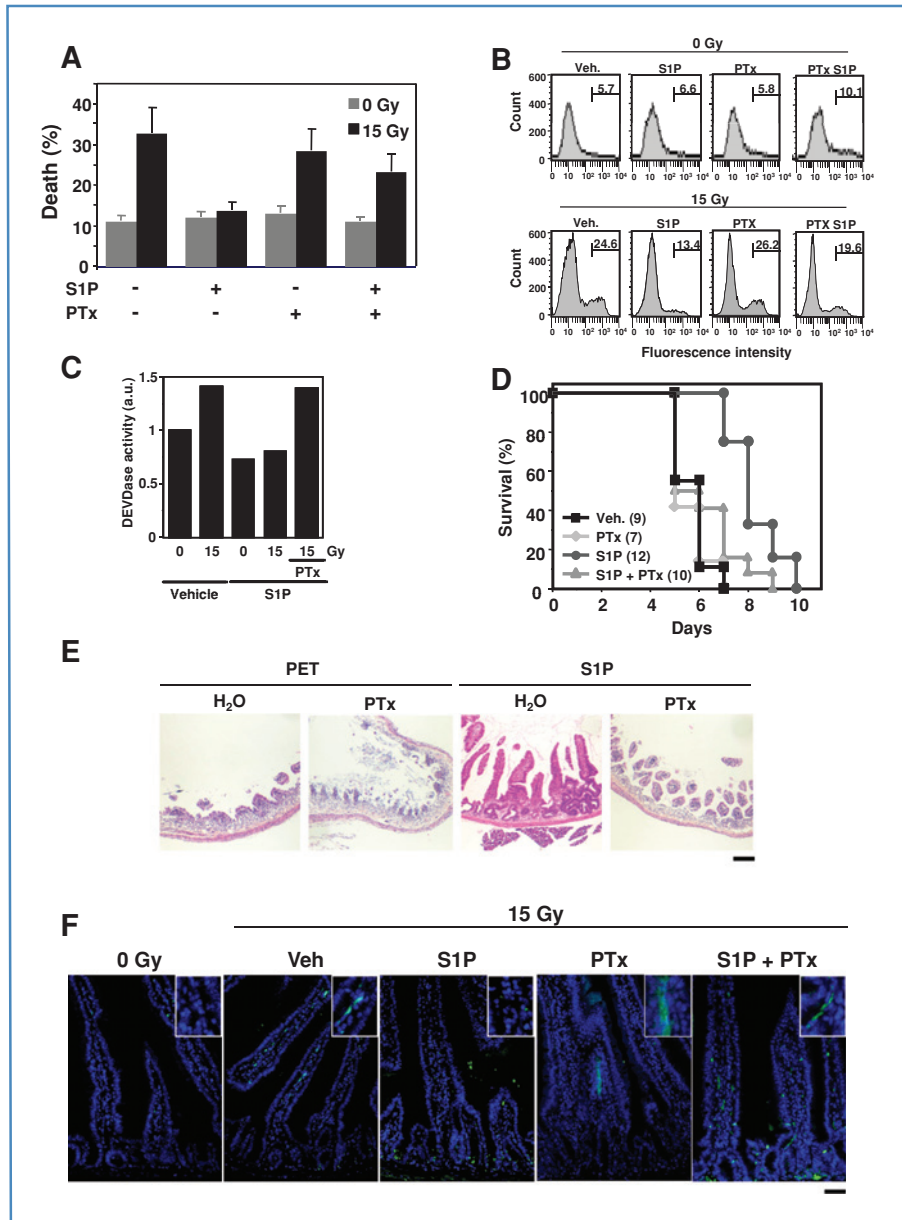
Figure 3. S1P does not reduce hematopoietic radiation toxicity. A, 1 of the 3 experiments showing alive (gray) and apoptotic (dark) T lymphocytes 48 hours after 15 Gy w/o S1P. T lymphocytes were detected by FACS with amcyan, apoptosis with FITC-Annexin V, and the whole-cell population with 7-AAD. B, percentage of CD3-positive apoptotic cells after 15 Gy w/o S1P (mean \pm SD, $n = 3$). C, 1 of the 3 experiments showing alive (gray) and apoptotic (dark) B lymphocytes after 15 Gy w/o S1P. Condition and staining are similar to A except APC-CD19 for B lymphocytes instead of CD3. D, amount of CD19-positive apoptotic cells after 15 Gy w/o S1P (mean \pm SD, $n = 3$). E, leukocytes counts in 15 Gy-irradiated and S1P-treated mice (mean \pm SEM, $n = 3$, $P < 0.01$ vs. sham-treated mice). F, survival curves of S1P-treated and/or BM-transplanted mice after 15 Gy. Number in parentheses indicates animals/group.

inhibits endothelial cell apoptosis within the intestinal villi (mean apoptosis: 1.6% after 16.95 Gy; ref. 21) as compared with those from irradiated wild-type mice observed by us ($11.3 \pm 0.3\%$ in wild-type mice after 15 Gy) and others (5, 6, 22), which proves that *Tie2Cre;bak1^{-/-};bax^{FL/-}* mouse model is not appropriate to evaluate BAX-mediated endothelial cell apoptosis and its association to the GI syndrome. Contrastingly, the present study shows reduced endothelial cell apoptosis within villi from S1P-treated mice after 15 Gy WBR ($3.7 \pm 0.5\%$) at a level comparable with that observed after bFGF treatment at the same dose ($3.2 \pm 0.4\%$; personal data). This inhibition of endothelial cell apoptosis by S1P is correlated with the prevention of the GI syndrome, which provides another proof of the crucial role

of endothelial apoptosis in intestinal necrosis, crypt shrinkage, and GI syndrome.

Despite an enhancement of crypt survival and an inhibition of crypt epithelial cell mitotic catastrophe by S1P (Fig. 2A and B), direct protection of irradiated epithelial cells by S1P seems to be excluded according to our *in vitro* studies using IEC-6 cells (Fig. 2C and D), as well as transformed intestinal T84, colonic tumor Caco2, and HCT116 epithelial cell lines (data not shown). As already described in a coculture model, irradiation of HMVEC endothelial cells in the presence of nonirradiated T84 epithelial cells induces mitotic arrest and apoptosis of the epithelial layer (23). Blocking radiation-induced endothelial cell apoptosis with S1P protects the epithelial compartment indirectly. Alternately, lisophosphatidic acid (LPA), a lipid

Figure 4. PTx pretreatment inhibits S1P-induced endothelial cell survival and small intestinal radioprotection. A–C, evaluation of apoptosis in PTx- and/or S1P-treated HMEC-1 24 hours after 15 Gy: (A) by floating cell count (mean \pm SD; $n = 3$), (B) by APO2.7 analysis ($n = 3$, 1 representative FACS analysis), and (C) by DEVDase assay ($n = 3$, 1 representative assay). D, survival curves of S1P- and/or PTx-treated mice after 15 Gy. Number in parentheses indicates animals/group. E, H&E-stained duodenum from agonal mice after 15 Gy w/o PTx and S1P. Scale bar, 200 μ m. F, apoptosis using FITC-TUNEL (green) and DAPI (blue) in duodenal sections from 15 Gy-irradiated and/or PTx- and S1P-treated mice. Scale bar, large picture 60 μ m, window 30 μ m.



functionally related to S1P, protects IEC-6 cells from radiation-induced death (24). Radiation-induced endothelial cell apoptosis and the GI syndrome were not inhibited by LPA or dihydrosphingosine-1-phosphate despite their capacity to bind to S1P receptors with a low affinity (Supplementary Fig. S1). The discrepancy of S1P radioprotection observed between the endothelium and the epithelium may be explained by the difference in cell death mechanisms. Endothelial cells die rapidly by a ceramide-dependent apoptosis, whereas epithelial cells are more subject to delayed mitotic death (25).

The GI syndrome is mainly related to endothelial and epithelial dysfunctions, whereas BM aplasia is triggered by the death of hematopoietic stem cell. Binding of extracellular S1P to its receptors has been reported to enhance trafficking

of T and B lymphocytes in the lymphoid system as well as their migration in nonimmune tissues (26). T and B lymphocytes were sensitive to radiation in a time-dependent manner, with no protection by S1P pretreatment (Fig. 3), which proves a lack of molecular redundancy in the S1P-mediated immune cell maturation and survival processes. Blood counts and histology of agonal mice show a lack of protection by S1P from radiation-induced leukopenia and BM aplasia, respectively. This was confirmed by the fact that mice injected with S1P and irradiated at 15 Gy were protected for more than 4 months by transplantation of fresh nonirradiated BM 16 hours post-irradiation.

The present study sheds new light on the mechanism underlying S1P radioprotection, which was largely unknown.

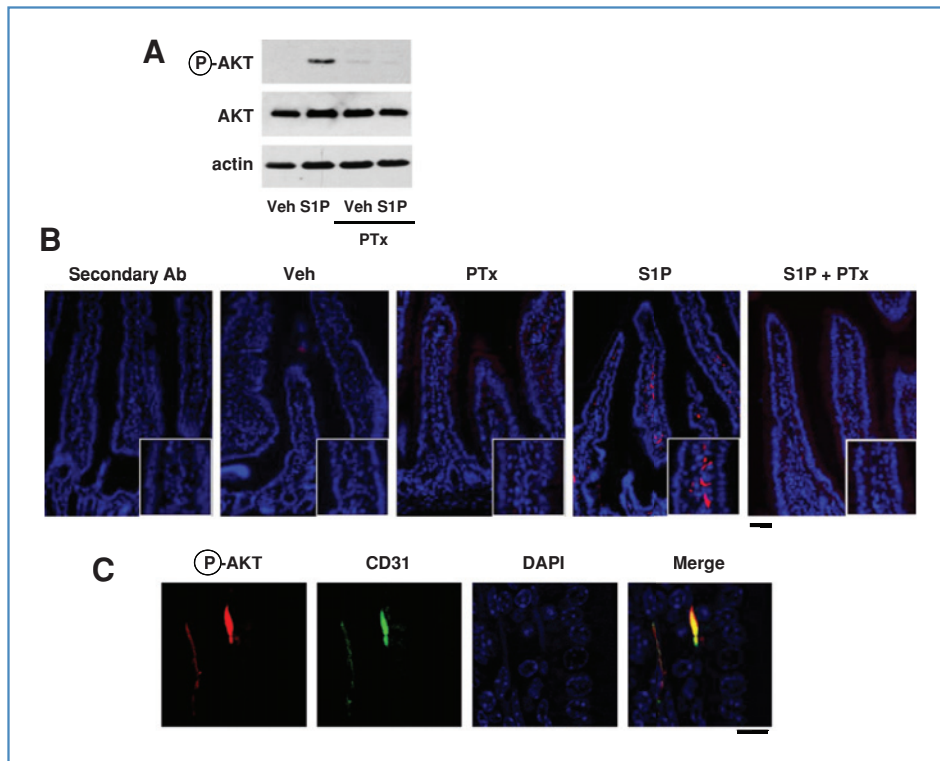


Figure 5. PTx pretreatment inhibits *in vitro* and *in vivo* S1P-induced phospho-AKT. A, phospho-AKT expression by Western blotting in HMEC-1–treated w/o PTx for 45 minutes and/or S1P for 15 minutes ($n = 3$, 1 representative blot). B, phospho-AKT immunostaining (red) and DAPI (blue) of duodenal sections from PTx- and/or S1P-treated mice. Scale bar, large picture 60 μm , window 30 μm . C, colocalization of the FITC-CD31 endothelial marker (green) and phospho-AKT (red) is shown by the yellow staining on the merge image. Scale bar, 10 μm .

S1P protection of oocytes from radiation- and doxorubicin-induced death (12, 19) was not inhibited by PTx, arguing for a, S1P-dependent intracellular protective pathway, at least in oocytes. Either intra- or extracellular S1P pathways have been considered to be involved in survival signaling in endothelial cells. Serum starvation–induced human umbilical vein endothelial cell (HUVEC) death is enhanced by inhibiting either the extracellular pathway through PTx treatment (27) or the intracellular pathway through overexpression of sphingosine kinase 1 (28). Our data support the involvement of the extracellular pathway in both *in vitro* and *in vivo* S1P-induced endothelial cell radioprotection (Fig. 4). S1P protection of endothelial cell apoptosis detected by APO2.7 in HMEC-1 or directly within the lamina propria was reversed by PTx pretreatment. Extracellular S1P has not been directly studied *in vivo* but has been indirectly investigated through the use of related agonist/antagonist to S1P receptors. The most studied drug is FTY720, a synthetic myriocin analogue that acts as a functional antagonist by internalizing S1P1 receptors, which are then degraded by the proteasome (29). FTY720 prevents S1P-mediated biological functions in HUVEC such as tumor angiogenesis and Ca^{2+} mobilization (30). Endothelial apoptosis has not been examined after the treatment with FTY720; however, knocking out the S1P1 or S1P3 receptors, using an antisense strategy, reverses S1P protection against serum deprivation–induced HUVEC death (16). Further investigations using S1P receptor transgenic models or specific inhibitors will better define mode of action of the S1P as a survival signal.

The PI3K/AKT couple is considered as a robust pro-survival mediator enforcing endothelial cell integrity (31). S1P

pretreatment of mice specifically induced AKT phosphorylation in endothelial cells within the lamina propria but not in the epithelial layer. Furthermore, *in vitro* and *in vivo* studies showed that AKT phosphorylation is under the control of the extracellular S1P pathway, as shown by the inhibition of S1P-induced phospho-AKT by PTx pretreatment (Fig. 5). The fact that pharmacologic inactivation of phospho-AKT blocked S1P-induced protection of the small intestines after irradiation (Fig. 6) strongly supports the hypothesis that the endothelial compartment plays a crucial role in the regulation of the fate of the small intestines after exposure to ionizing radiation. Recently, treatments with insulin growth factor-1 (IGF-1) and bFGF have been shown to activate AKT phosphorylation in crypt columnar cells and inhibit PUMA and p53-mediated GI damage (32). Because S1P receptors are expressed in the intestinal epithelial mucosa (personal data), we cannot exclude the fact that S1P activate AKT in crypt epithelial stem cells. However, no crypts or epithelial cells were shown to be positive for phospho-AKT staining in S1P-treated mice. This apparent discrepancy may be due to the kinetics of AKT phosphorylation. Although S1P induces phosphorylation in endothelial cells within 15 minutes, AKT is activated in crypt columnar cells 4 hours after IGF-1 and bFGF treatment. Different pharmacologic strategies succeeded in inhibiting AKT activation and enhancing tumor endothelial cell radiosensitivity (33), with no observation on normal tissue radiotoxicity. In our study, the fact that phospho-AKT staining was untraceable in small intestine sections from untreated mice and AKTi treatment did not modulate death of 15 Gy–irradiated mice could be considered as a first proof

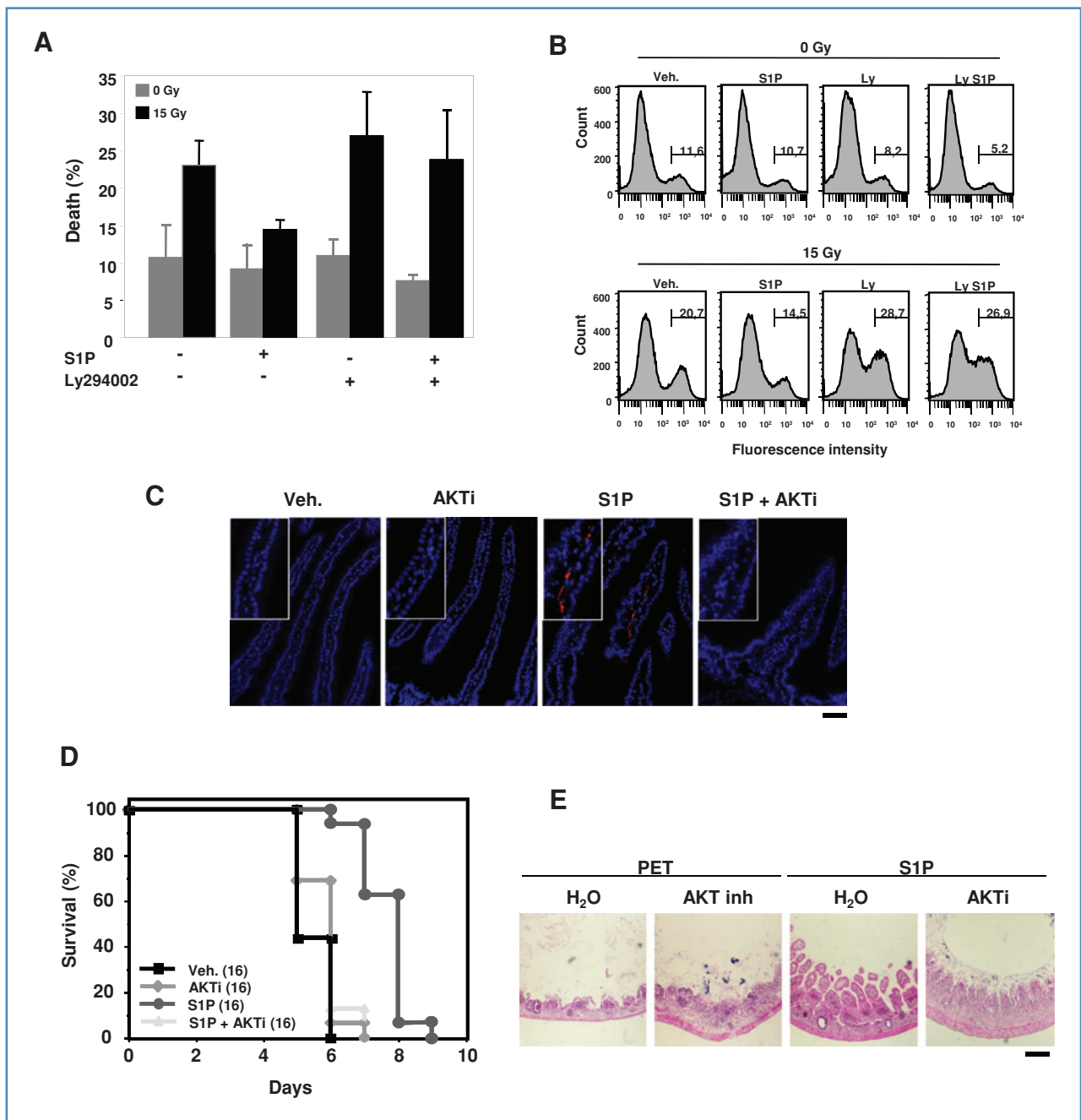


Figure 6. AKTi inhibits S1P-induced endothelial cell survival and small intestines radioprotection. A and B, evaluation of apoptosis in Ly294002- and/or S1P-treated HMEC-1 24 hours after 15 Gy: (A) by floating cell count (mean \pm SD; $n = 3$) and (B) by APO2.7 analysis ($n = 3$, one representative FACS analysis). C, phospho-AKT immunostaining (red) and DAPI (blue) of duodenal sections treated w/o AKTi and S1P. Scale bar, large picture 60 μ m, window 30 μ m. D, survival curves of S1P- and/or AKTi-treated mice after 15 Gy. Number in parentheses indicates animals/group. E, H&E-stained duodenum from agonal mice after 15 Gy w/o AKTi and S1P. Scale bar, 250 μ m.

of the specificity of the AKT inhibition strategy in tumor but not in normal tissue endothelium.

In conclusion, we showed that S1P is a relevant bioactive lipid that can inhibit the GI syndrome through the promotion of endothelial cell survival. S1P is known for its pleiotropic roles in biological functions, such as proliferation,

adhesion, inhibition of permeability, and lymphocyte maturation. Additional studies, either on the pharmacologic modulation of sphingosine kinase or sphingosine lyase activity, which changes the intracellular levels of S1P, or on the characterization of the S1P receptor(s) involved in the survival signal transduction cascade, are necessary to better

define a class of drugs conferring endothelial protection with few side effects.

Disclosure of Potential Conflicts of Interest

No potential conflicts of interest were disclosed.

References

- Paris F, Fuks Z, Kang A, Capodiceci P, Juan G, Ehleiter D, et al. Endothelial apoptosis as the primary lesion initiating intestinal radiation damage in mice. *Science* 2001;293:293-7.
- Potten CS, Owen G, Roberts SA. The temporal and spatial changes in cell proliferation within the irradiated crypts of the murine small intestine. *Int J Radiat Biol* 1990;57:185-99.
- Pritchard DM, Potten CS, Korsmeyer SJ, Roberts S, Hickman JA. Damage-induced apoptosis in intestinal epithelia from bcl-2-null and bax-null mice: Investigations of the mechanistic determinants of epithelial apoptosis *in vivo*. *Oncogene* 1999;18:7287-93.
- Burdelya LG, Krivokrysenko VI, Tallant TC, Strom E, Gleiberman AS, Gupta D, et al. An agonist of toll-like receptor 5 has radioprotective activity in mouse and primate models. *Science* 2008;320:226-30.
- Cho CH, Kammerer RA, Lee HJ, Steinmetz MO, Ryu YS, Lee SH, et al. COMP-Ang1: a designed angiopoietin-1 variant with nonleaky angiogenic activity. *Proc Natl Acad Sci U S A* 2004;101:5547-52.
- Rotolo JA, Maj JG, Feldman R, Ren D, Haimovitz-Friedman A, Cordon-Cardo C, et al. Bax and Bak do not exhibit functional redundancy in mediating radiation-induced endothelial apoptosis in the intestinal mucosa. *Int J Radiat Oncol Biol Phys* 2008;70:804-15.
- Harada-Shiba M, Kinoshita M, Kamido H, Shimokado K. Oxidized low density lipoprotein induces apoptosis in cultured human umbilical vein endothelial cells by common and unique mechanisms. *J Biol Chem* 1998;273:9681-7.
- Cuvillier O, Pirianov G, Kleuser B, Vanek PG, Coso OA, Gutkind S, et al. Suppression of ceramide-mediated programmed cell death by sphingosine-1-phosphate. *Nature* 1996;381:800-3.
- Igarashi J, Michel T. Sphingosine 1-phosphate and isoform-specific activation of phosphoinositide 3-kinase beta. Evidence for divergence and convergence of receptor-regulated endothelial nitric-oxide synthase signaling pathways. *J Biol Chem* 2001;276:36281-8.
- Xia P, Wang L, Gamble JR, Vadas MA. Activation of sphingosine kinase by tumor necrosis factor-alpha inhibits apoptosis in human endothelial cells. *J Biol Chem* 1999;274:34499-505.
- Lee MJ, Van Brocklyn JR, Thangada S, Liu CH, Hand AR, Menzeleev R, et al. Sphingosine-1-phosphate as a ligand for the G protein-coupled receptor EDG-1. *Science* 1998;279:1552-5.
- Morita Y, Perez GI, Paris F, Miranda SR, Ehleiter D, Haimovitz-Friedman A, et al. Oocyte apoptosis is suppressed by disruption of the acid sphingomyelinase gene or by sphingosine-1-phosphate therapy. *Nat Med* 2000;6:1109-14.
- Sun X, Shikata Y, Wang L, Ohmori K, Watanabe N, Wada J, et al. Enhanced interaction between focal adhesion and adherens junction proteins: involvement in sphingosine 1-phosphate-induced endothelial barrier enhancement. *Microvasc Res* 2009;77:304-13.
- Moriue T, Igarashi J, Yoneda K, Nakai K, Kosaka H, Kubota Y. Sphingosine 1-phosphate attenuates H₂O₂-induced apoptosis in endothelial cells. *Biochem Biophys Res Commun* 2008;368:852-7.
- Zheng DM, Kitamura T, Ikejima K, Enomoto N, Yamashina S, Suzuki S, et al. Sphingosine 1-phosphate protects rat liver sinusoidal endothelial cells from ethanol-induced apoptosis: role of intracellular calcium and nitric oxide. *Hepatology* 2006;44:1278-87.
- Kwon YG, Min JK, Kim KM, Lee DJ, Billiar TR, Kim YM. Sphingosine 1-phosphate protects human umbilical vein endothelial cells from serum-deprived apoptosis by nitric oxide production. *J Biol Chem* 2001;276:10627-33.
- Bonnaud S, Niaudet C, Pottier G, Gaugler MH, Millour J, Barbet J, et al. Sphingosine-1-phosphate protects proliferating endothelial cells from ceramide-induced apoptosis but not from DNA damage-induced mitotic death. *Cancer Res* 2007;67:1803-11.
- Greenspon J, Li R, Xiao L, Rao JN, Marasa BS, Strauch ED, et al. Sphingosine-1-phosphate protects intestinal epithelial cells from apoptosis through the Akt signaling pathway. *Dig Dis Sci* 2009;54:499-510.
- Paris F, Perez GI, Fuks Z, Haimovitz-Friedman A, Nguyen H, Bose M, et al. Sphingosine 1-phosphate preserves fertility in irradiated female mice without propagating genomic damage in offspring. *Nat Med* 2002;8:901-2.
- Withers HR, Elkind MM. Microcolony survival assay for cells of mouse intestinal mucosa exposed to radiation. *Int J Radiat Biol Relat Stud Phys Chem Med* 1970;17:261-7.
- Kirsch DG, Santiago PM, di Tomaso E, Sullivan JM, Hou WS, Dayton T, et al. p53 controls radiation-induced gastrointestinal syndrome in mice independent of apoptosis. *Science* 2010;327:593-6.
- Qiu W, Carson-Walter EB, Liu H, Epperly M, Greenberger JS, Zambetti GP, et al. PUMA regulates intestinal progenitor cell radiosensitivity and gastrointestinal syndrome. *Cell Stem Cell* 2008;2:576-83.
- Gaugler MH, Neunlist M, Bonnaud S, Aubert P, Benderitter M, Paris F. Intestinal epithelial cell dysfunction is mediated by an endothelial-specific radiation-induced bystander effect. *Radiat Res* 2007;167:185-93.
- Deng W, Balazs L, Wang DA, Van Middlesworth L, Tigyi G, Johnson LR. Lysophosphatidic acid protects and rescues intestinal epithelial cells from radiation- and chemotherapy-induced apoptosis. *Gastroenterology* 2002;123:206-16.
- Merritt AJ, Allen TD, Potten CS, Hickman JA. Apoptosis in small intestinal epithelial from p53-null mice: evidence for a delayed, p53-independent G2/M-associated cell death after gamma-irradiation. *Oncogene* 1997;14:2759-66.
- Rosen H, Goetzl EJ. Sphingosine 1-phosphate and its receptors: an autocrine and paracrine network. *Nat Rev Immunol* 2005;5:560-70.
- Kimura T, Sato K, Kuwabara A, Tomura H, Ishiura M, Kobayashi I, et al. Sphingosine 1-phosphate may be a major component of plasma lipoproteins responsible for the cytoprotective actions in human umbilical vein endothelial cells. *J Biol Chem* 2001;276:31780-5.
- Limaye V, Li X, Hahn C, Xia P, Berndt MC, Vadas MA, et al. Sphingosine kinase-1 enhances endothelial cell survival through a PECAM-1-dependent activation of PI-3K/Akt and regulation of Bcl-2 family members. *Blood* 2005;105:3169-77.
- Oo ML, Thangada S, Wu MT, Liu CH, Macdonald TL, Lynch KR, et al. Immunosuppressive and anti-angiogenic sphingosine 1-phosphate receptor-1 agonists induce ubiquitinylation and proteasomal degradation of the receptor. *J Biol Chem* 2007;282:9082-9.
- LaMontagne K, Littlewood-Evans A, Schnell C, O'Reilly T, Wyder L, Sanchez T, et al. Antagonism of sphingosine-1-phosphate receptors

Grant Support

Electricité de France, La Ligue Nationale Contre le Cancer, Association pour la recherche sur le Cancer, and Institut National du Cancer.

Received 06/07/2010; revised 08/23/2010; accepted 09/16/2009; published OnlineFirst 11/30/2010.

- by FTY720 inhibits angiogenesis and tumor vascularization. *Cancer Res* 2006;66:221–31.
31. Shiojima I, Walsh K. Role of Akt signaling in vascular homeostasis and angiogenesis. *Circ Res* 2002;90:1243–50.
32. Qiu W, Leibowitz B, Zhang L, Yu J. Growth factors protect intestinal stem cells from radiation-induced apoptosis by suppressing PUMA through the PI3K/AKT/p53 axis. *Oncogene* 2010;29:1622–32.
33. Edwards E, Geng L, Tan J, Onishko H, Donnelly E, Hallahan DE. Phosphatidylinositol 3-kinase/Akt signaling in the response of vascular endothelium to ionizing radiation. *Cancer Res* 2002;62:4671–7.

Cancer Research

The Journal of Cancer Research (1916–1930) | The American Journal of Cancer (1931–1940)

Sphingosine-1-Phosphate Activates the AKT Pathway to Protect Small Intestines from Radiation-Induced Endothelial Apoptosis

Stéphanie Bonnaud, Colin Niaudet, François Legoux, et al.

Cancer Res 2010;70:9905-9915. Published OnlineFirst November 30, 2010.

Updated version	Access the most recent version of this article at: doi: 10.1158/0008-5472.CAN-10-2043
Supplementary Material	Access the most recent supplemental material at: http://cancerres.aacrjournals.org/content/suppl/2010/11/30/0008-5472.CAN-10-2043.DC1

Cited articles	This article cites 33 articles, 16 of which you can access for free at: http://cancerres.aacrjournals.org/content/70/23/9905.full.html#ref-list-1
-----------------------	--

Citing articles	This article has been cited by 9 HighWire-hosted articles. Access the articles at: /content/70/23/9905.full.html#related-urls
------------------------	---

E-mail alerts	Sign up to receive free email-alerts related to this article or journal.
----------------------	--

Reprints and Subscriptions	To order reprints of this article or to subscribe to the journal, contact the AACR Publications Department at pubs@aacr.org .
-----------------------------------	--

Permissions	To request permission to re-use all or part of this article, contact the AACR Publications Department at permissions@aacr.org .
--------------------	---